

# Modeling of Ultra Wide Band Channels Within Vehicles

Paul Richardson, Weidong Xiang, *member, IEEE* and Wayne Stark, *Fellow, IEEE*

**Abstract**— This paper aims to lay a solid foundation for the application of ultra wide band (UWB) radio in vehicle environments by exploring the characteristics of UWB channels within a vehicle. A comprehensive measurement campaign was conducted to gather a set of channel impulse responses of UWB links within and outside an armored vehicle. Based on the experimental data, the channel's temporal characteristics, path loss and capacities are analyzed. The distributions of delay spread and amplitudes of multipath signals are also studied, showing correspondence with the IEEE 802.15.3a UWB channel model. The UWB channels within the vehicle are then modeled by extracting relevant cluster and ray arrival rates and cluster and ray decay factors.

**Index Terms**—UWB; Channel Model.

## I. INTRODUCTION

Ultra wideband (UWB) radio has attracted a great deal of research interest and applied for a variety of commercial and military applications recently. The extremely wide bandwidth promises tremendous channel capacity and makes UWB radio immune to conventional narrowband interferences. A major focus on UWB radio applications in the commercial sector has for wireless personal area network (WPAN) offering data rates up to 480Mb/s over short distances of 4-10 meters.

Recently there has been interest in the use of UWB in both military and commercial vehicles. The developers of commercial vehicles are interested in replacing certain segments of conventional wired control network with a wireless communications system. The amount of cabling required in a modern automobile could exceed 4km in some cases [7] and the costs associated with developing, installing, and maintaining this amount of cabling per vehicle is becoming prohibitive. By eliminating a significant percentage of the total signal cables in a vehicle, developers can reap big savings in manufacturing, maintaining and new model developing.

Military users have also expressed an interest in short range (< 200m) communications in proximity to the vehicle. The goal is to provide the crew with connection to the vehicle when they are dismounted. Dismounted operations in urban and industrialized environments are of special interest because of the hazards associated with them.

The replacement of conventional wired links with wireless connections in vehicular systems presents a number of challenges regarding system reliability and safety. UWB radio is regarded as a competitive candidate to address these challenges due to its superior properties: resilience to narrowband interference and extremely low radiation power. Similarly, for dismounted military operations in proximity to the vehicle, UWB radio is difficult to be jammed and detected. Moreover, the fine delay capability can provide accurate range determination.

These emerging applications for UWB presents new channel environments that have not been extensively studied. The new channel environments include the inside of both commercial and military vehicles and various short-range outdoor environments in proximity to the vehicle. The major research focus of UWB channel models has been predominantly in the area of high data rate, short range commercial applications. The IEEE 802.15.3a work group has defined a UWB indoor channel model for the 4m-10m range [5] based on the clustering effects first reported by Saleh and Valenzuela [8]. Many efforts have focused on the UWB channel for indoor environments because of the tremendous commercial potential that exists [2-12]. The effects of human beings in sparse and dense multipath environments are described in [13]. The propagation of UWB radio signals through different building materials are studied in [14]. The UWB channels in watertight ship compartments are explored in [15] and UWB outdoor channels in forested environments are discussed in [16].

In this paper, we study the UWB channels within a vehicle and outdoors in proximity to the vehicle in an industrial environment. The objective is to gain the channel impulse responses (CIRs) of UWB channels in these environments and to compare the results with those derived from the IEEE 802.15.3a channel model developed for indoor environments.

The paper is arranged as follows. The experiment set up is described in section 2. In section 3 we measure the temporal characteristics of UWB channels and compare with those from the IEEE 802.15.3a model. Section 4 discusses channel capacity and path loss. Conclusions are given finally.

Manuscript received March 1, 2004.

Paul Richardson is with the University of Michigan, Dearborn, Dearborn, MI, 48128 USA (richarpc@umich.edu)

Weidong Xiang is with the University of Michigan, Dearborn, Dearborn, MI, 48128 USA (phone: 313.593.5525; xwd@umich.edu)

Wayne Stark is with the University of Michigan, Ann Arbor, Ann Arbor, MI 48109 USA (stark@eecs.umich.edu)

II. THE UWB TESTBED AND EXPERIMENTS

The vehicle selected for this study is an armored military vehicle. An industrial environment is selected because it is a challenging environment for dismounted military operations. The industrial site selected is a manufacturing building at the U.S. Army Tank-Automotive Research Center (TARDEC), in Warren, MI.

The PulsON 200 Evaluation Kit (EVK) from the Time Domain Corporation is adopted in the test. The EVK generates 0.24ns wide pulses at a rate of 9.6MHz. The pulse signal occupies a bandwidth of 2.9GHz centralized at 4.55GHz. The EVK adopts time-hopping scheme to deliver the information in packets. Each packet contains a preamble and control information.

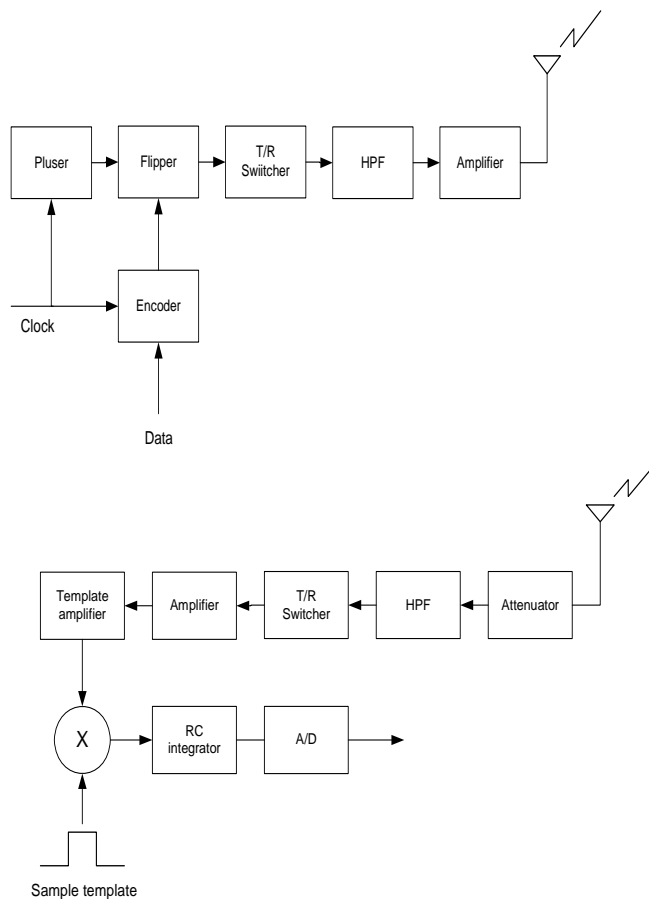


Fig. 1 The diagrams of the transmitter (up) and receiver (bottom) of the PulsON 200 EVK

Figure 1 depicts the block diagram of the EVK. At transmitter, the pulser generates a pulse stream and passes it to a flipper module that controls each pulse’s polarity. The binary bit stream is fed into a time-hopping encoder which assigns pseudo random time offsets to trigger the flipper. The pulse polarities are decided by the values of bits. The time-hopping code lengths are 16 or 32 bits. The encoded pulse stream is then shaped by a high-pass filter to fit the spectrum mask specified by the Federal Communications Committee (FCC). Finally, the pulse stream is amplified and radiated to the air. At receiver, the pulse signals are first filtered and per-

amplified. During the acquisition, the pulse signals are correlated to a template waveform matched to certain time offsets and polarities. The results of the correlator are integrated and used to alarm the acquisition if the accumulated value is greater than a given threshold. After acquisition, the EVK captures 100ns waveform of input pulse signal at a 3ps interval. The captured data, known as a waveform scan, is then saved as a file to the hard driver of a computer for further processing. A CLEAN algorithm [17] is used to de-convolve the CIR. An example of waveform scan and estimated CIR are given in Fig.2.

The overall dimensions of the vehicle under study are 6.4m long, 2.5m wide, and 2.3 m high. The vehicle is made of steel alloy and has only a few hard ended glass view ports and rubber sealed hatches from which radio waves could leak. The inside of the vehicle contains many metallic obstructions and large metal surfaces, effectively creating a reverberation chamber. Figure 3 shows the top and side views of the vehicle. Both the infrastructure and ad hoc configurations were studied. The infrastructure configuration consisted of 12 remote points (TXi) and an access point (RX). 3-4 measurements were taken for each link in the cases of one person (for data collecting) and a crew of five to quantify the impact of personnel.

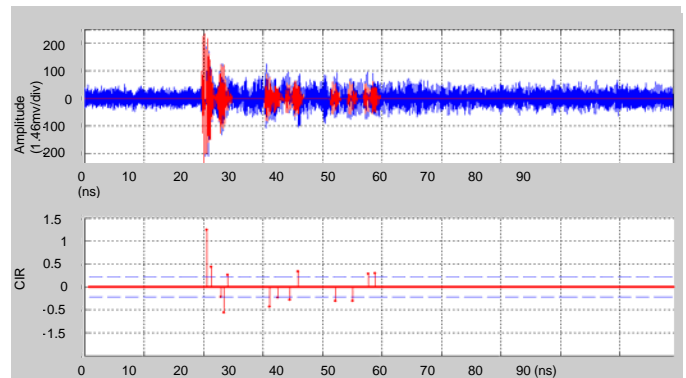


Fig. 2 An example of waveform scan (top) and estimated CIR (bottom) (TX 5 to RX)

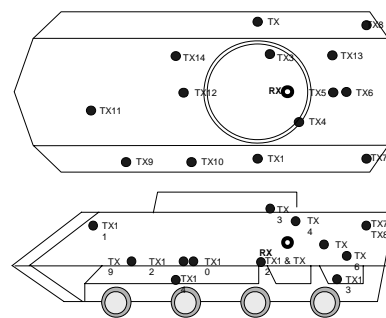


Fig.3 The top and side views of the vehicle and the positions of RX and TX1-TX12

The next set of measurements was collected in an outdoor industrial environment in proximity to the vehicle. This environment was surrounded on two sides by a manufacturing building with aluminum sides. There were seven semi-tractor trailers, a large refuse container (dumpster), three cars, and a tractor. There were also four small trees, less than 5m in height and an enclosed bus stop. The maximum measurement range over the width and length of the vehicle was 32m and 68m.

The outdoor measurements were divided into two classes. The first set of 22 measurements was performed in proximity to the vehicle (3m-8m) to explore the effects of transmitting in the area of the RF shadow of the vehicle. These measurements were conducted to gain insight into vehicle blind spots. The top and side views of this configuration were shown in Fig.4. LOC1-4 were the transmitting nodes and MOB1-12 were remote receiving nodes. The transmitting nodes were positioned on the front, top, side, and rear of the vehicle to estimate blind spots and coverage area from different antenna positions for remote points in the RF shadow of the vehicle. The remote nodes were placed at positions on the ground, about 2m lower than the transmitters. The second set of 17 measurements was taken at greater distances (13.9m to 45.1m) to capture the path losses and capacity. Figure 5 depicts the measurement positions.

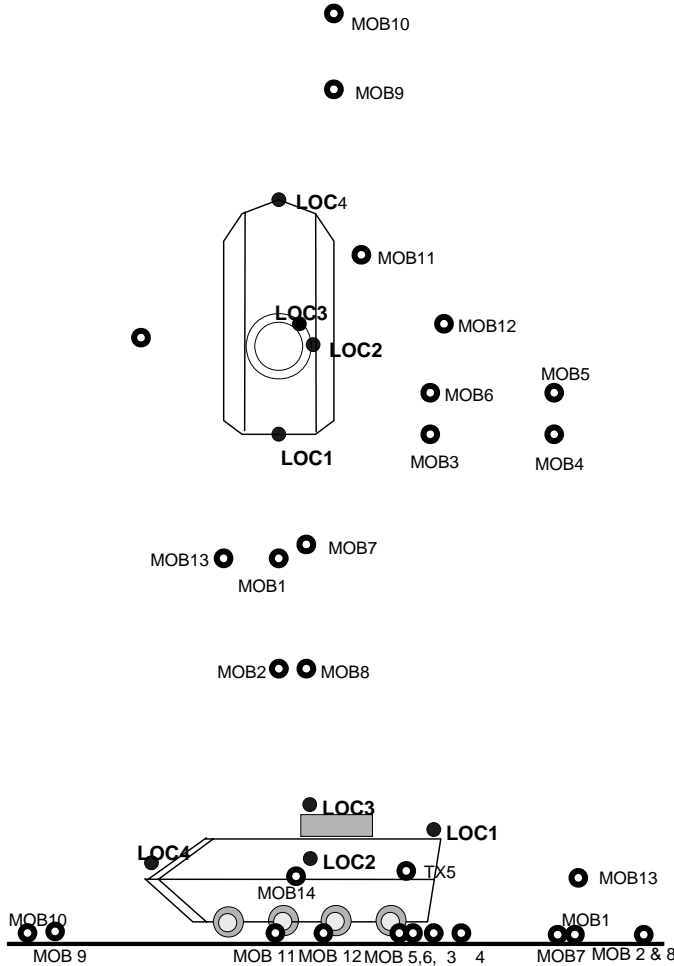


Fig.4 Top and side views of the measurement positions in proximity to the vehicle

### III. TEMPORAL PARAMETERS OF CAPTURED CIRs AND COMPARISON TO THE IEEE 802.15.3a MODEL

From the CIR, we can determine mean delay spread,  $\bar{\tau}$ , RMS delay spread,  $\tau_{rms}$  and number of MPC,  $N_p$ . Based on these parameters, we could extract corresponding parameters of the 802.15.3a model. This allows us to compare the experimental results with those derived from theoretical model.

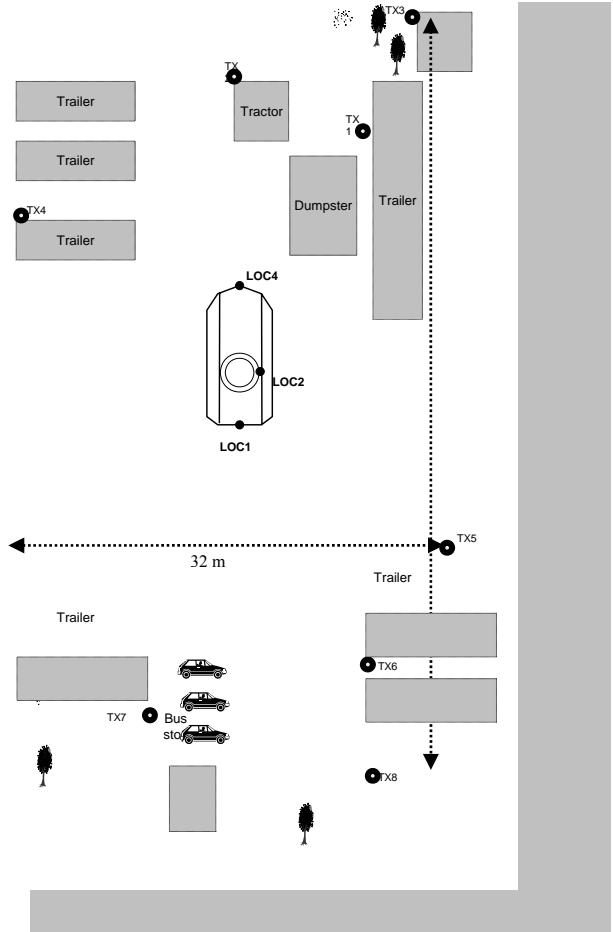


Fig. 5 The positions of measurement points in an industrial environment industrial environment

There are significant delay spreads for in-vehicle channels due to the small dimensions of the vehicle and the large amount of metal surfaces within the vehicle. The in-vehicle channels can be distinguished by being LOS or NLOS links and by having one or five occupants. Figure 6 depicts the mean values of  $\bar{\tau}$ ,  $\tau_{rms}$ , and  $N_p$  for the four in-vehicle links. It is expected that the crew would absorb or block energy leading that the delay spread for the case of one occupant is larger than that of five occupants. For the case of five occupants,  $\bar{\tau}$  is lowered by 5.15ns and  $\tau_{rms}$  decreases by 6.36ns. Because of the large number of obstructions within the vehicle,  $N_p$  is generally great for NLOS channels regardless of the path lengths. For LOS channels, the LOS component and a small number of significant MPCs dominate the

received signal. The difference in  $N_p$  for the case of five occupants is smaller than that of one occupant, indicating the fact that the occupants block or absorb reflected energy.

The outdoor measurements taken in proximity to the vehicle were intended to measure vehicle blind spots and channel conditions in the area of the vehicle's RF shadow. The majority of the channels have  $\tau_{rms}$  less than 8ns and many less than 2ns indicating that the multipath components die out rapidly. Figure 7 depicts the mean values of  $\bar{\tau}$ ,  $\tau_{rms}$ , and  $N_p$  for LOS and NLOS links. Generally, the LOS links have small  $\bar{\tau}$ ,  $\tau_{rms}$ , and  $N_p$ . For larger distances, the NLOS links average 19 significant MPCs. This is attributable to the industrial environment with many large reflective objects. Maximum range measured for a LOS link was 45.1m and 35.5m for a NLOS link.

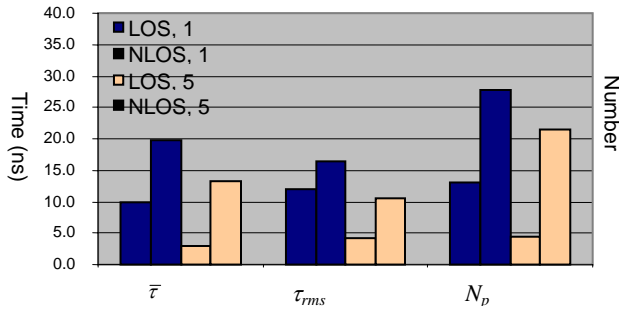


Fig. 6 Average values of  $\bar{\tau}$ ,  $\tau_{rms}$ , and  $N_p$  for the four in-vehicle channels

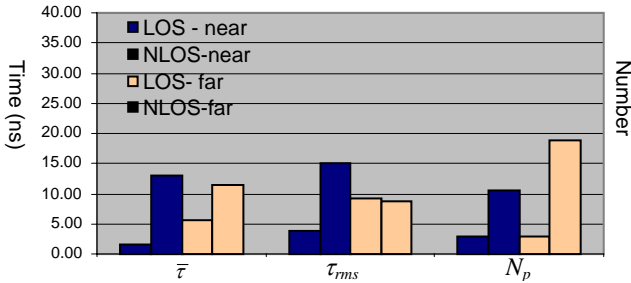


Fig. 7 Average values of  $\bar{\tau}$ ,  $\tau_{rms}$ , and  $N_p$  for outdoor channels

Figure 8 graphs the distributions of  $\tau_{rms}$ , and  $N_p$  for the indoor and outdoor channels, respectively. Inside the vehicle,  $\tau_{rms}$  are concentrated around the mean values while  $N_p$  tends to be more uniformly distributed. In the outdoor environment, the distribution for  $\tau_{rms}$  that are weighted towards shorter durations and the distribution of  $N_p$  is significantly weighted toward fewer MPCs.

The IEEE 802.15.3a work group has defined a model for UWB channels in indoor environments [5,6]. The model predicts the arrival of MPC as clusters with each cluster consisting of some number of rays. In this model the cluster and ray arrival follow a Poission distribution. The amplitudes

of MPCs follow a lognormal distribution. The CIR consists of a LOS signal if exists and many resolvable multipath signals with corresponding gains and arrival times, normally expressed as,

$$h(t) = \sum_{l=0}^L \sum_{k=0}^K \alpha_{k,l} \delta(t - T_l - \tau_{k,l}) \quad (2.1)$$

where  $T_l$  is the delay spread of  $l$ -th cluster,  $\tau_{k,l}$  is the delay spread of  $k$ -th array relative to  $l$ -th cluster.  $\alpha_{k,l} = p_{k,l} \beta_{k,l}$  is the gain of the  $k$ -th array of  $l$ -th cluster where  $p_{k,l}$  is an equiprobable distribution of  $\pm 1$ , and  $20 \log_{10}(\beta_{k,l}) \sim N(\mu_{k,l}, \sigma^2)$  expresses the lognormal distributed shadow fading.  $L$  and  $K$  are the numbers of clusters and arrays, respectively.

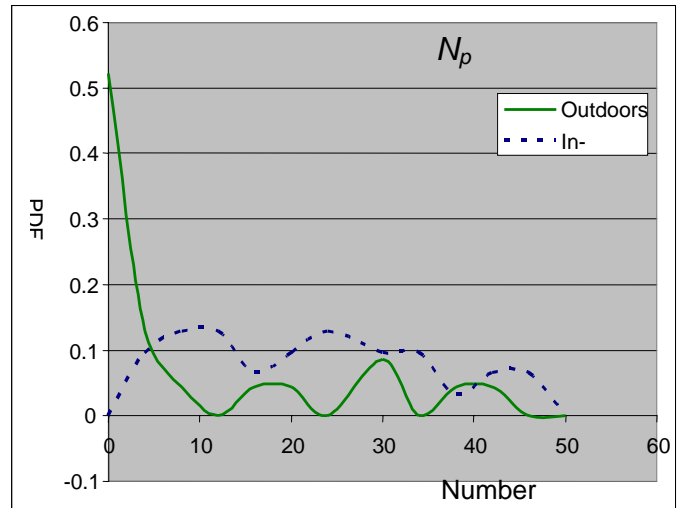
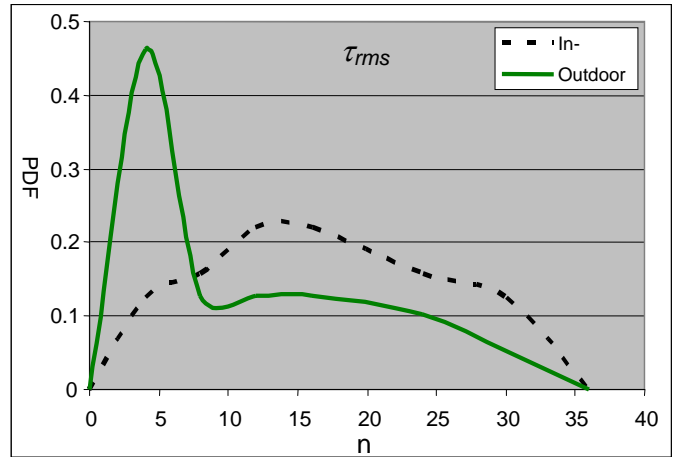


Fig.8 The distributions of  $\tau_{rms}$  and  $N_p$  spread for in-vehicle and outdoor channels

We compute the model parameters of cluster and ray arrival rates ( $\Lambda$  and  $\lambda$ ) and cluster and ray decay parameters ( $\Gamma$  and  $\gamma$ ) for the measured data using a scan search method that

attempts to minimize the sum of mean square errors between measured and simulated  $\bar{\tau}$ ,  $\tau_{rms}$ , and  $N_p$  to a given threshold.

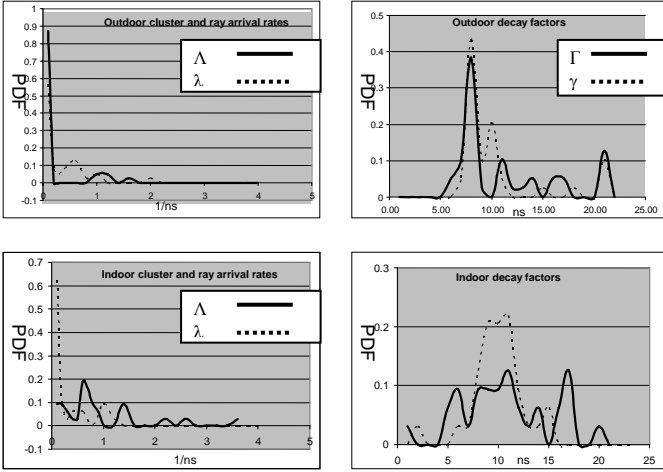


Fig. 9 The distributions of model parameters for in-vehicle and outdoor channels

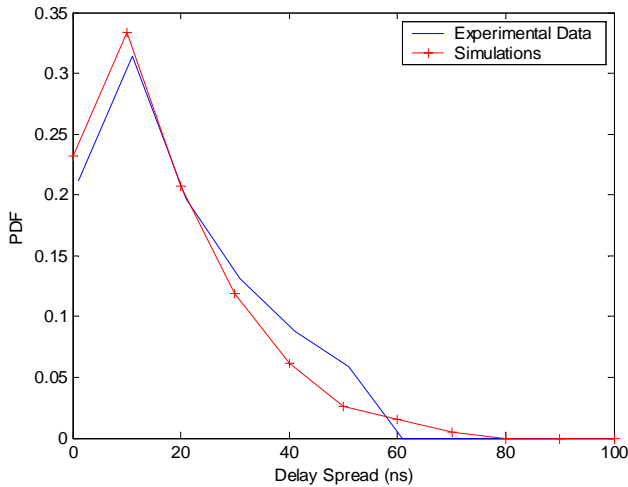


Fig.10 The comparison of the distributions of RMS delays for simulation and experimental data

The distributions of the model parameters calculated from the measured data are given in Fig.9. The cluster and ray arrival rates of the NLOS channels are significantly higher than that of LOS channels. This is consistent with the temporal parameters from the measured data which indicated the LOS channels have a LOS component and only a few dominant MPCs while the NLOS channels have many more significant MPCs. For in-vehicle measurements, the model parameters show the cluster and ray decaying faster for the case of five occupants versus the case of one occupant, which is consistent with the measured delay spreads. Interestingly the model parameters also show the LOS channels have cluster and ray decay factors that are greater than those of the NLOS channels. The similarity of the parameters of NLOS links with one or five occupants is quite rational. For NLOS links, path multipath components are mainly decided the

propagation environment. The presence of five occupants does not evidently chance the propagation environment which is mainly decided by the metal configuration of vehicle.

In order to assess the accuracy of the 802.15.3a UWB model in representing the measured in-vehicle and outdoor channels, we generated  $\tau_{rms}$  and the normalized amplitude of MPC using the model and compared with the measured data. Figure 10 and 11 shows the distributions of  $\tau_{rms}$  and the normalized amplitude for measured and simulated data, respectively. The simulated data has similar distributions in terms of  $\tau_{rms}$  and normalized amplitude. We could approximately extend the 802.15.3a model to the vehicular environments.

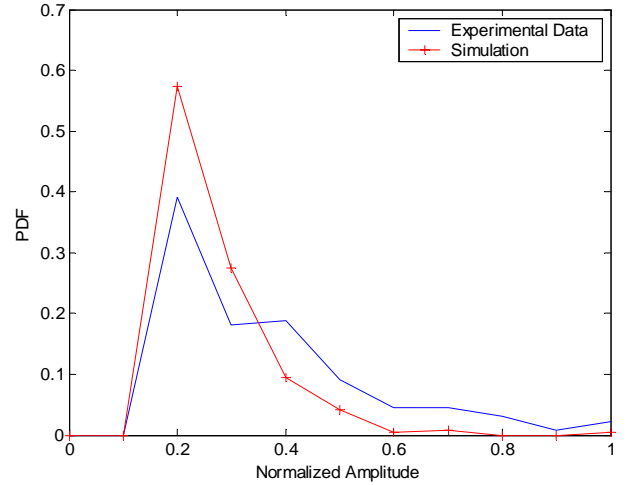


Fig.11 The comparison of the distributions of normalized amplitudes of MPC for simulation and experimental data

#### IV. ANALYSIS OF PATH LOSS AND CAPACITY

The path loss, referred to as  $L_S$ , represents the energy dissipation during the propagation, exclusives of the impact of antenna and receiver and is normally given as,

$$L_S = P_T + G_T + G_R - P_R + L_R \quad (3.1)$$

where  $P_R$  is the received signal power at the output of the receive link after the signal passing through the amplifiers, mixer, and analog-to-digital converter,  $G_T$ ,  $G_R$  are the transmitter and receiver antenna gains, respectively.  $L_R$  represents the sum of receiver gains, insert attenuations and mismatches. In order to estimate  $L_R$ , the testbed is calibrated by measuring the CIR of a LOS channel in free space (actual an open filed) with a span of 1 meter. In the EVK, we have  $G_T = G_R = 2.1\text{dB}$ ,  $P_T = -15\text{dBm}$ , and  $L_S = 20\log_{10}\left(\frac{c}{4\pi df_g}\right) = 45\text{dB}$ , where  $d=1\text{m}$  and the geometric center frequency is given as  $f_g = \sqrt{f_L f_H} = 4.243\text{GHz}$ . Thus  $L_R$  is derived for free space conditions as  $L_R = 55.8\text{dB}$ .

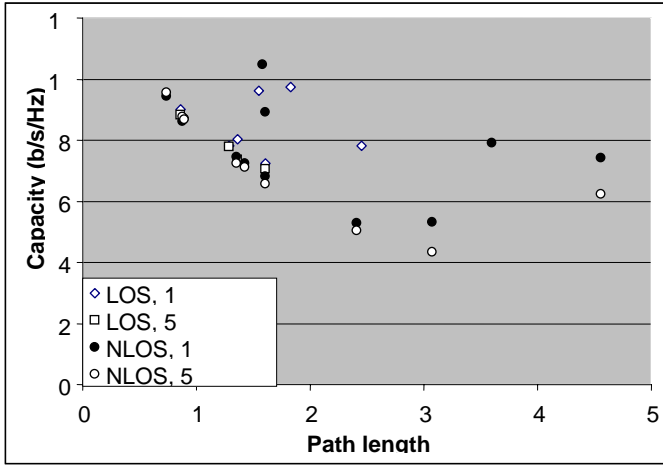


Fig. 12 Capacity versus distance for channels within the vehicle

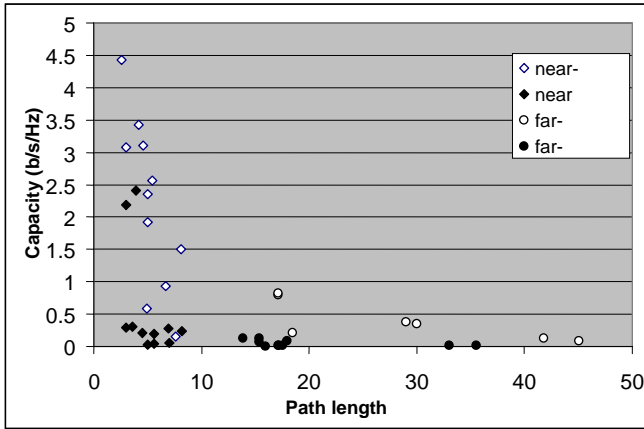


Fig. 13 Capacity versus distance for outdoor channels in an industrial environment

After  $L_R$  becomes known, the received signal power  $P_R$  varies linearly with the path loss and is given as:

$$P_R = \frac{1}{N} \sum_{i=0}^N |H(f_i)|^2 \quad (3.2)$$

The capacity could be derived by using the channel frequency response,  $H(f)$ , obtained from the CIR. The capacity is calculated for an ideal transmitter that could transmit at  $-41\text{dBm/MHz}$  over the entire  $2.9\text{GHz}$  spectrum. We assume that the receiver is capable of recovering all resolvable multipath components. The whole bandwidth of  $3.1\text{-}6\text{GHz}$  is divided into 2900 sub-channels which has  $1\text{MHz}$  bandwidth and is regarded as fat. Then the channel capacity is given as,

$$C = \sum_{i=1}^N \log_2 \left( 1 + \frac{P_T |H(f_i)|^2}{N_0 \Delta f} \right) \Delta f \quad (3.3)$$

and

$$H(f_i) = \sum_{l=0}^L \sum_{k=0}^K \alpha_{k,l} e^{-j2\pi f_i \tau_{k,l}} \quad i = 1 \dots N \quad (3.4)$$

where  $N=2900$ ,  $P_T=-41\text{dBm/MHz}$ .

Inside the vehicle, the path loss does not show an evident tendency to increase with distance. For in-vehicle channels, small differences in path lengths would imply that distance dependent path loss is not a significant factor. Rather we would expect to see the effects of the obstructions and the presence of crew to dominant path loss.

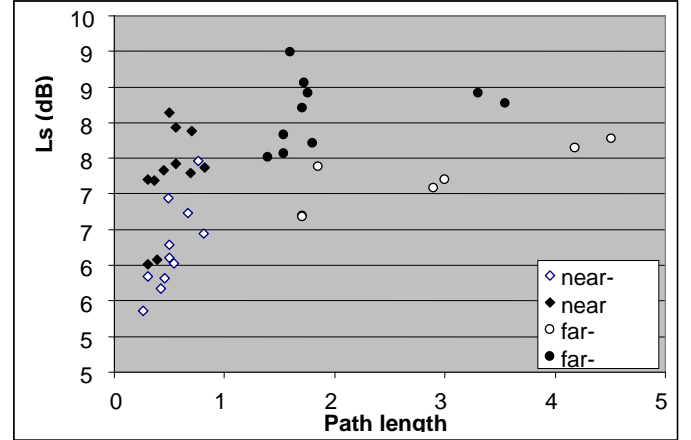


Fig. 14 Path loss distributions versus distance for outdoor channels in an industrial environment

Inside the vehicle, the capacity for LOS channel with 5 occupants does show a monotonic relationship with distance. For the remaining cases, the relationship between capacity and distance are random. Figure 12 depicts capacity versus the distance for the channel within vehicle.

Figure 13 and 14 shows the capacity and path loss versus the distance for the outdoor channels, respectively. For the outdoors environments, the distance dependent path loss is evident for LOS channels over longer distances ( $>15\text{m}$ ). However, the same can not be said for NLOS channels of the same length. We attribute this to the industrial environment that creates a rich multipath environment generating many additional multipath components. The path loss for NLOS channels near the vehicles demonstrates random distribution, indicating effects of RF propagation shadow.

The channel capacity for the LOS channels far from the vehicle exhibit pronounced distance dependent capacity. The NLOS channels have low capacities regardless of distances. The capacities of the LOS channel in the shadow area show a sensitivity to distance.

## V. CONCLUSION

Within the vehicles, the UWB radio is capable to provide high data rates up to Gbits/s through either the LOS or NLOS channels in the cases with or without crew. For the outdoor environment, the UWB channels at distances of up to  $45\text{m}$

still contain significant capacity. In an industrial environment with many large metal surfaces, UWB radio can offer a data rate of tens of Mbits/s through NLOS channels at distances up to 35m.

It is verified that the IEEE 802.15.3a UWB model could provide reasonably accurate simulation results for UWB channels in vehicular environments.

#### REFERENCES

- [1] M. Ghavami, L. Michael and R. Kohno, *Ultra wide signals and systems in communications engineering*, Wiley and Sons, 2004
- [2] J. Choi, and W. Stark, "Performance of ultra-wideband communications with suboptimal receivers in multipath channels," *IEEE JSAC*, vol. 20, pp.1754-1766, Dec., 2002
- [3] R. Cramer, R. Scholtz and M. Win, 'Evaluation of an ultra-wide-band propagation channel,' *IEEE Transactions on AP*, vol. 50, pp. 561-570, May, 2002
- [4] M. Win and R. Scholtz, "Characterization of ultra-wide bandwidth wireless indoor channels: a communication-theoretic view," *IEEE JSAC*, vol. 20, pp.1613-1627, Dec., 2002
- [5] J. Foerster, "Channel modeling sub-committee report final", *IEEE P802.15-02/368r5-SG3a*, Dec., 2002
- [6] M. Pendergrass, "Empirically based statistical ultra-wideband channel model," *IEEE P802.15-02/240-SG3a Sep.*, 2004
- [7] P. Richardson, A. Elkateeb and L. Sieh, "Intra-vehicle computer networks—emerging trends, protocols, and obstacles," *International Engineering Consortium Annual Communications Review*, vol. 57, pp. 757-786, 2004
- [8] A. Saleh and R. Valenzuela, "A statistical model for indoor multipath propagation," *IEEE JSAC*, vol. 5, pp.128-137, Feb. 1987
- [9] S. Ghassemzadeh, L. Greenstein, A. Kavcic, T. Sveinsson and V. Tarokh "UWB indoor path loss model for residential and commercial buildings," *IEEE VTC Fall 2003*,
- [10] J. Foerster, M. Pendergrass, and A. Molisch, "A channel model for ultra wideband indoor communication," *International Symposium on Wireless Personal Multimedia Communication*, Oct., 2003
- [11] D. Cassioli, M. Win, and A. Molisch, "The ultra-wide bandwidth indoor channel: from statistical model to simulations," *IEEE JSAC*, vol. 20, pp.1247-1257, Aug. 2002
- [12] F. Zhu, Z. Wu, and C. Nassar, "Generalized fading channel model with application to UWB," *Ultra Wideband Systems and Technologies Conference*, pp. 13-17, May 2002
- [13] T. Welch, R. Musselman, B. Emessiene, P. Gift, D. Choudhury, D. Cassadine and S. Yano, "The effects of the human body on UWB signal propagation in an indoor environment" *IEEE JSAC*, vol. 20, pp.1778-1782, Dec. 2002
- [14] R. Lao, J. Tarnq, and C. Hsiao, "Transmission coefficients measurement of building materials for UWB systems in 3-10GHz," *Vehicular Technology Conference*, Spring 2003. vol. 1, pp.22-25, April 2003
- [15] "Shipboard propagation measurements," *Time Domain Corp.*, Technical Report, July 2001
- [16] G. Schiavone, P. Wahid, R. Palaniappan, J. Tracy, E. van Doorn, and B. Lonske, "Outdoor propagation analysis of ultra wide band signals," *IEEE Antennas and Propagation Society International Symposium*, 2003, vol. 2, pp.22-27 June 2003
- [17] R. Scholtz, R. Cramer, and M. Win, "Evaluation of the propagation characteristics of ultra-wideband communication channels," *Antennas and Propagation Society International Symposium*, vol. 2, pp.21-26, June 1998

**Paul C. Richardson** is an Associate Professor in the Department of Electrical and Computer Engineering, University of Michigan, Dearborn. Dr. Richardson is a Principal Investigator for ultrawideband applications with the U.S. Army Research Development, and Engineering Center, Warren, MI and a consultant for the United States Marine Corps regarding command and control networks. He received the B.S.E. degree in computer engineering, the M.S.E.

degree in computer and electrical engineering, and the Ph.D. degree in systems engineering, all from Oakland University, Rochester, MI. His interests include embedded real-time systems, vehicular networks and communications systems, and ultrawideband applications.

**Weidong Xiang** received his M.S.E.E. and Ph.D. degrees from Tsinghua University, Beijing, China, in 1996 and 1999, respectively. From 1999 to 2004 he worked as a post-doctoral fellow and then research scientist in the Software Radio Laboratory (SRL) at Georgia Institute of Technology, Atlanta, USA. In September 2004 he joined the ECE Department, University of Michigan-Dearborn as an assistant professor. His research interests include high-speed wireless LAN prototype integrating MIMO, OFDM, software radio, and smart antenna, wireless access for vehicular environments (WAVE), Ultrawide band (UWB), and real-time wireless control network.

**Wayne Stark** received the B.S. (with highest honors), M.S., and Ph.D. degrees in electrical engineering from the University of Illinois, Urbana in 1978, 1979, and 1982 respectively. Since September 1982 he has been a faculty member in the Department of Electrical Engineering and Computer Science at the University of Michigan, Ann Arbor where he is currently Professor. From 1984-1989 he was Editor for *Communication Theory* of the *IEEE Transactions on Communication* in the area of Spread-Spectrum Communications. He was involved in the planning and organization of the 1986 International Symposium on Information Theory which was held in Ann Arbor, Michigan. He was selected by the National Science Foundation as a 1985 Presidential Young Investigator. He was the principal investigator of a Army Research Office Multidisciplinary University Research Initiative (MURI) project on Low Energy Mobile Communications. His research interests are in the areas of coding and communication theory, especially for spread-spectrum and wireless communication networks. Dr. Stark is a member of Eta Kappa Nu, Phi Kappa Phi and Tau Beta Pi and a Fellow of the IEEE. Dr. Stark received the 2002 IEEE Milcom Technical Achievement Award for sustained technical contributions to military communications.